Optical Materials 51 (2016) 190–193

Contents lists available at ScienceDirect

Optical Materials

journal homepage: www.elsevier.com/locate/optmat

Hybrid waveguiding structure in $LiTaO_3$ crystal fabricated by direct femtosecond laser writing

Chen Cheng [a], Yuechen Jia [a], Javier R. Vázquez de Aldana [b], Yang Tan [a], Feng Chen [a,*]

[a] School of Physics, State Key Laboratory of Crystal Materials and Key Laboratory of Particle Physics and Particle Irradiation (MOE), Shandong University, Jinan 250100, China
[b] Laser Microprocessing Group, Universidad de Salamanca, Salamanca 37008, Spain

ARTICLE INFO

Article history:
Received 5 August 2015
Received in revised form 9 November 2015
Accepted 26 November 2015
Available online 1 December 2015

Keywords:
Optical waveguides
Femtosecond laser micromachining
Lithium tantalate crystal
Polarization-selective devices

ABSTRACT

A hybrid waveguiding structure has been fabricated in a *z*-cut lithium tantalate ($LiTaO_3$) crystal wafer by direct femtosecond laser writing. Due to the laser-induced anisotropic modifications of the extraordinary and ordinary refractive indices (n_e and n_o) of $LiTaO_3$ crystal, the structure exhibits polarization-sensitive guiding features along vertical and horizontal orientations. Based on this feature, circularly-polarized light beam can be converted to vertically-/horizontally-polarized ones (i.e., TE and TM), with approximately 1:1 power splitting ratio. The well-guided performance of the polarization-sensitive structure shows the potential for integration with existing light signals to realize all-optical information processing.

1. Introduction

Dielectric crystals possess versatile features for a wide range of applications as electro-optical modulation, lasing, nonlinear frequency conversion, information storage, etc. In photonics, based on the waveguide technology, various miniature devices, such as directional couplers, beam splitters, and ring resonators, have been extensively applied in diverse areas, e.g., the optical telecommunications, quantum computing, sensing for atmosphere or biology [1–11]. Guided-wave optical devices based on dielectric crystals enable the combination of the compact geometries and the bulk features, receiving both passive and active applications. For example, $LiNbO_3$-based waveguide devices have been utilized for electro-optical modulation, signal amplification, and frequency conversion [12–15], and the rare-earth-ion-doped YAG crystalline waveguides have become promising miniature light sources for integrated photonic chips [16–19]. Although a number of techniques have been developed to produce waveguides in various dielectric crystals, it still contains considerable difficulty in the process of the fabrication, due to the complexity of crystalline structures, bulk chemical/physical features, and the limitations of each technique applied to different crystals. The direct femtosecond laser writing has recently become a powerful technique to perform 3D micromachining of diverse materials for a broad range of applications [20–23]. High-intensity femtosecond laser pulses allow the micro-modification of the material matrix with an extreme precision through strong-field ionization processes. In particular, it has become a unique technique to fabricate waveguides in optical materials since 1996 [24]. In glasses, intense femtosecond laser pulses usually induce positive changes of the refractive index ($\Delta n > 0$) at the laser-irradiated areas. This feature enables direct 3D microfabrication of various devices [4,25]. Significantly different, femtosecond lasers typically induce negative index changes ($\Delta n < 0$) at the irradiated areas of dielectric crystals [20]. Although it is considerably difficult to find appropriate irradiation conditions, one could in principle generate anisotropic changes of n_o and n_e, by applying femtosecond laser modification with suitable parameters. For example, the Jena group realized positive n_e and negative n_o in $LiNbO_3$ by using direct laser writing [26]. Most dielectric crystals are birefringent, which enables polarization-sensitive light propagation in the crystals. For example, the light will be decomposed into ordinary and extraordinary waves, experiencing a different refractive index of crystal along particular orientations. This has been widely applied, for instance, in prism bulks with diverse configurations. (e.g., Wollaston, Glan–Taylor prisms). In the process of fabrication, a lattice-breakdown effect, which is induced by the femtosecond laser writing, causes severe damage of the crystalline matrix, usually results in a decrease of both extraordinary and ordinary indices. With this feature, it is possible to implement the splitting of one light beam into two beams with orthogonal polarizations in a "straightforward" way, i.e., the beams with ordinary and extraordinary indices propagate along different pathways. Lithium tantalate ($LiTaO_3$), whose

* Corresponding author.
E-mail address: drfchen@sdu.edu.cn (F. Chen).

http://dx.doi.org/10.1016/j.optmat.2015.11.043
0925-3467/

features are somehow similar to $LiNbO_3$, exhibits birefringence and tremendous potential in electro-optic and nonlinear optics application. In crystalline waveguide platforms, the construction of waveguide pairs that support separating guidance of TE and TM modes (hereby referring to them by the corresponding refractive index, n_o or n_e in z-cut $LiTaO_3$ crystal, respectively) with a certain spatial separation could offer more opportunities to achieve applications. In addition, for beam splitting purpose, the laser-induced guiding cores of the TE and TM polarized light must not be spatially overlapped (no superposition). In this work, a hybrid structure containing a combination of two separate guiding cores for n_o and n_e has been fabricated in a z-cut $LiTaO_3$ crystal wafer. Such a hybrid structure could be considered as a 'marriage' of a waveguide pair with one of positive changes of the refractive index (classified into Type-I waveguiding core) and depressed cladding (hereafter referring to Type-III guiding core geometry in this work; the related modification of the low-index laser-induced tracks is also accepted as Type-II structure) geometries [20]. The guiding properties, including guiding modal profiles, polarized features, and losses, of these Type-I and -III waveguides have been investigated independently. Through such a hybrid guiding structure, a light beam with circular polarization is separated into two independent light beams with TE- and TM-polarization. The power-split ratio of output TE and TM polarized light is nearly 1:1.

2. Experimental procedures

A z-cut $LiTaO_3$ single crystal wafer was cut into dimensions of $15(x) \times 10(y) \times 1(z)\,mm^3$ and optically polished. The laser writing of the structure was implemented by using the facility at University of Salamanca, Spain. An amplified Ti:Sapphire femtosecond laser (Spitfire, Spectra Physics) that delivered linearly-polarized pulses with a temporal duration of 120 fs, a central wavelength of 795 nm and a repetition rate of 1 kHz, was used as the laser source. The beam was focused by a 20× microscope objective and the energy on sample was reduced to 0.4 μJ (measured after the objective) by using a set of $\lambda/2$ waveplate and linear polarizing cube, and a calibrated neutral density filter. The laser irradiation was controlled with a mechanical shutter. The sample was placed on an XYZ micro-positioning stage that allowed scanning the sample at constant velocity (0.5 mm/s) along the y-direction while irradiating from the surface of $15 \times 10\,mm^2$ with the femtosecond pulses at certain depth beneath the surface (~150 μm). As a result, a tubular-like cladding structure (3 μm lateral separation of adjacent parallel tracks) with a diameter of ~20 μm and an oblate circular cross-sectional geometry has been fabricated, and all the produced damage tracks are divided into two well-differentiated parts: one section (~17 μm-long) shows a soft damage, another one (~12 μm-long) exhibits a more severe damage with defects formation. Among which, the weakly damaged parts of several parallel damage tracks results in a large-area Type-I waveguide. This region may confine long wavelengths, but only for the extraordinary component ($\Delta n_e > 0$) [26–28]. In order to confine the ordinary component ($\Delta n_o < 0$) in a separated region, a Type-III cladding structure is necessary. By adjusting the focal depth of the femtosecond laser, another waveguide structure with circular shape was implemented. A gap is generated between Type-I and Type-III cores, in which light field cannot be confined due to inadequate refractive index contrast for waveguiding (See Fig. 1(a)). When the incident light enters the gap area, it will split and be coupled into Type-I or Type-III waveguide regions ultimately, depending on the polarization of the light. Fig. 1(b) depicts the working mechanism of the waveguides obtained in this work, in which an input circular polarized light beam hits the gap area and is separated into two beams with orthogonal polarized orientations. Fig. 1(c) shows the schematic plot of the waveguide fabrication process.

Optical characterization of the waveguides was performed through an end-face coupling system. A linearly-polarized CW solid-state laser at wavelength of 1064 nm was utilized as the light source. When needed, the linear polarization of input light would be converted to circular one via a $\lambda/4$ waveplate. The input light beam was coupled into the structure by a 20× microscope objective lens. Another microscope objective lens was used as the outcoupler, through which the output light was collected and imaged by a CCD camera. The total losses (including propagation losses and coupling losses) of the photonic structures were determined by directly measuring the light powers (by powermeters) from the input and output end-faces.

The mismatch coefficient (C_{GP}) between launched Gaussian laser mode and the propagation modal profile in waveguide can be expressed as [29]

$$C_{GP} = \frac{1}{2}\left(\frac{\varepsilon_0}{\mu_0}\right)\int_A E_G^* E_P\, dA \tag{1}$$

where E_G refers to the incident Gaussian field and E_P represents the propagating mode though hybrid waveguide. The coupling losses due to the mismatch can be obtained by the following expression:

$$Loss = -10\log\left(|C_{GP}|^2\right) \tag{2}$$

Fresnel reflection losses at each waveguide–air interface were also considered, as follows:

$$R = \left(\frac{n_2 - n_1}{n_1 + n_2}\right)^2 \tag{3}$$

where n_1 and n_2 are refractive indices of two interface media.

3. Results and discussion

Fig. 2(a)–(c) depict the measured output nearly-field intensity profiles, with circularly polarized 1064 nm input light launched into Type-III, gap and Type-I areas, respectively. An additional linearly polarizer is inserted into the end-face coupling system (before the detector, not shown in Fig. 1(c)) to investigate the polarization features of the output beams. The results show that, firstly, in the case of the circularly polarized light is launched into the Type-III core area, the light beam leaving channel Type-III area maintains the original circular polarization (Fig. 2(a)); secondly, in the case of the same light beam is launched into the gap area, TE- and TM-polarized light leaves from Type-III and -I channels (Fig. 2(b)), respectively; at last, for light launched into the Type-I area, a linearly TM polarized light beam could be guided and detected at the output facet of the system (Fig. 2(c)).

In addition, we calculate the modal profiles of the waveguides numerically based on the estimation of the laser-induced refractive index changes. By assuming a step-index profile, the refractive index modification can be estimated by the numerical aperture method through the following equation [30]

$$\Delta n_{o,e} \approx \frac{\sin^2\theta_m}{2n_{o,e}} \tag{4}$$

where θ_m is the maximum incident angular deflection at which no transmitted power change occurs ($\theta_m = 3.5°$ with a difference of 0.3° between both polarizations). The calculated index modification $\triangle n_{o,e} \approx 1 \times 10^{-3}$ for the laser-written $LiTaO_3$ waveguides. The near-field intensity profiles corresponding to the propagation of hybrid waveguide output at 1064 nm are calculated by the FD-BPM algorithm (Rsoft®Beam PROP), which are shown in Fig. 2(d–e), which are in good agreements with the experimental data.

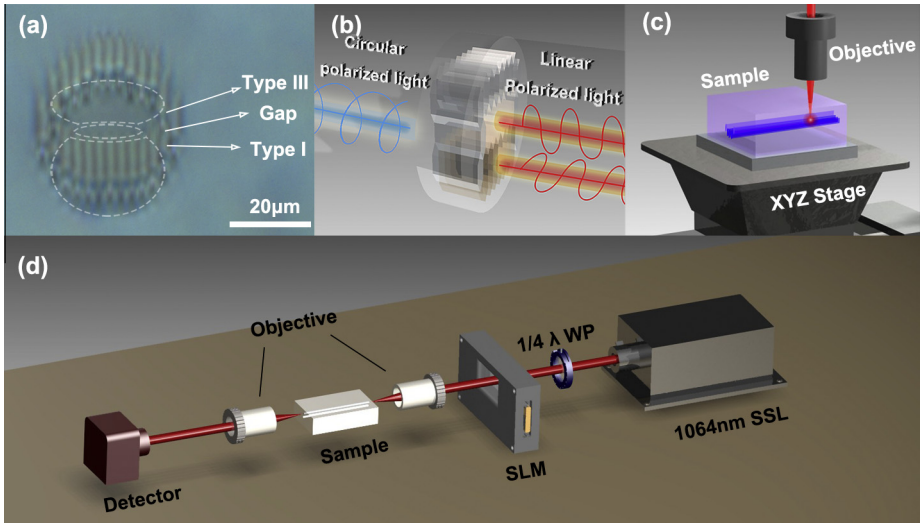

Fig. 1. The microscope image of the cross section of the hybrid waveguide and the waveguiding area distribution (a). The artwork of the conversion from circular polarized light into two orthogonal linear polarized light beams (b). Schematic plot of the fabrication process with the femtosecond laser (c). An arrangement of end-face coupling system (d).

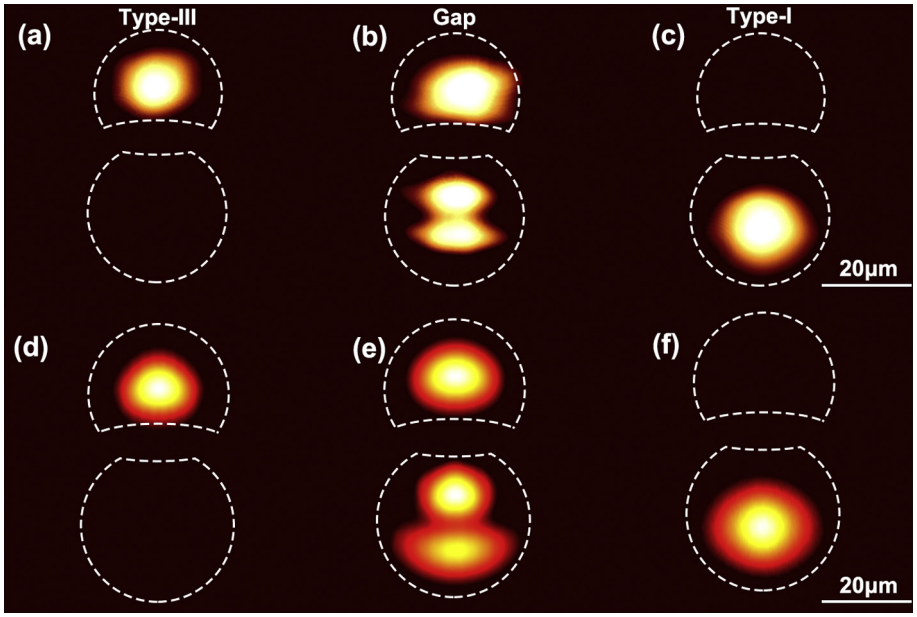

Fig. 2. (a–c) distribution of near-field by injecting circularly polarized light at 1064 nm into Type-III, gap and -I, respectively; (d–f) the near-field intensity profiles simulated corresponding to the propagation of demultiplexer output.

During the simulation, Δn_e is positive for the Type-I tracks and Δn_o is negative for Type-III tracks (Fig. 3(a) (n_o) and 3(b) (n_e)). To obtain thorough information of polarization effects of both waveguide channels, the all-angle light transmission along the transverse plane is measured with 6 mW 1064-nm light launched in two waveguide channels (Fig. 3(c)).

With the end-face coupling system, the measured total losses (including propagation losses and coupling losses) at 1064 nm were ~−3.09 dB and ~−2.26 dB for TE- (in the Type-III channel) and TM-polarized-light (in the Type-I channel), respectively.

The coupling losses can be ultimately calculated by the FD-BPM algorithm (Rsoft®Beam PROP) (~−1 dB for Type-I and -III cores). The Fresnel reflection is −0.61 dB at each waveguide–air interface. Above all, for the 1 cm-long hybrid waveguide sample, the propagation losses are estimated to be as low as ~0.04 dB/cm (Type-I) and 0.87 dB/cm (Type-III), respectively.

In the case of incident circularly polarized light into the gap area, the obtained splitting ratio was measured to be 1:1.037 (TE:TM), which is close to the ideal 1:1 ratio. The discrepancy is induced by the different attenuations of the Type-I and -III waveguides.

4. Conclusion

In summary, we have fabricated a hybrid waveguide of polarized sensitivity by direct femtosecond laser writing in a *z*-cut $LiTaO_3$ crystal. The laser induced anisotropic changes of n_o and n_e in the irradiated regions enable polarization-sensitive guidance in different parts of the designed structure. With this advantage, the hybrid waveguide splits the input circularly polarized light beam into TE and TM linear polarized beams that propagate through separated cores with a power ratio of 1:1, as a bridge

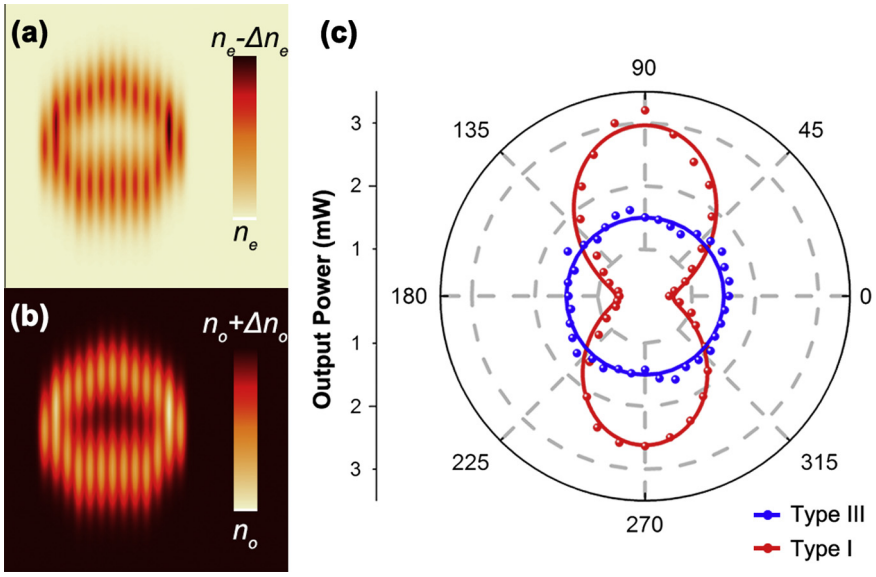

Fig. 3. Simulation of refractive index distributions of n_o and n_e (a, b); All-angle light transmission along the transverse plane at 1064 nm (c).

between two integrated optical systems constructed with different polarizations. An input beam with circular polarization is separated into the beams with different linear polarizations, which suggests the potential of the femtosecond laser written $LiTaO_3$ hybrid waveguides for all-optical applications. Finally, we would point out that the $LiTaO_3$ crystal in this work is a *z*-cut sample, which enables further poling periodically for nonlinear applications.

Acknowledgements

The work is supported by the National Natural Science Foundation of China (No. 11274203), Junta de Castilla y León under project SA086A12-2, and Ministerio de Economía y Competitividad (under project FIS2013-44174-P), Spain.

References

[1] D.N. Nikogosyan, Nonlinear Optical Crystals: A Complete Survey, Springer, New York, 2005.
[2] T. Meany, L.A. Ngah, M.J. Collins, A.S. Clark, R.J. Williams, B.J. Eggleton, M.J. Steel, M.J. Withford, O. Alibart, S. Tanzilli, Laser Photon. Rev. 8 (2014) L42–L46.
[3] S. Campbell, R.R. Thomson, D.P. Hand, A.K. Kar, D.T. Reid, C. Canalias, V. Pasiskevicius, F. Laurell, Opt. Express 15 (2007) 17146–17150.
[4] R. Osellame, G. Cerullo, R. Ramponi (Eds.), Femtosecond-Laser Micromachining: Photonic and Microfluidic Devices in Transparent Materials, Springer, New York, 2012.
[5] L. Gui, B.X. Xu, T.C. Chong, I.E.E.E. Photon, Technol. Lett. 16 (2004) 1337.
[6] D.G. Rabus, Integrated Ring Resonators, Springer, New York, 2007.
[7] G.A. Torchia, A. Rodenas, A. Benayas, E. Cantelar, L. Roso, D. Jaque, Appl. Phys. Lett. 92 (2008) 111103.
[8] B. Albrecht, P. Farrera, X. Fernandez-Gonzalvo, M. Cristiani, H. de Riedmatten, Nat. Commun. 5 (2014) 3376.
[9] S.Y. Yang, A.Q. Liu, L.K. Chin, X.M. Zhang, D.P. Tsai, C.L. Lin, C. Lu, G.P. Wang, N.I. Zheludev, Nat. Commun. 3 (2012) 651.
[10] R. Mary, D. Choudhury, A.K. Kar, IEEE J. Sel. Top. Quant. Electron. 20 (2014) 1–13.
[11] J. Siebenmorgen, T. Calmano, K. Petermann, G. Huber, Opt. Express 18 (2010) 16035–16041.
[12] Y. Liao, Y. Cheng, Z.H. Zhou, F. He, H.Y. Sun, J. Song, X.S. Wang, Z.Z. Xu, K. Sugioka, K. Midorikawa, Opt. Lett. 33 (2008) 2281–2283.
[13] G.A. Torchia, C. Mendez, I. Arias, L. Roso, A. Rodenas, D. Jaque, Appl. Phys. B 83 (2006) 559–563.
[14] S. Ringleb, K. Rademaker, S. Nolte, A. Tunnermann, Appl. Phys. B 102 (2011) 59–63.
[15] S. Nolte, M. Will, J. Burghoff, A. Tünnermann, Appl. Phys. A 77 (2003) 109–111.
[16] Y.C. Jia, C. Cheng, J.R.V. de Aldana, G.R. Castillo, B.D. Rabes, Y. Tan, D. Jaque, F. Chen, Sci. Rep. 4 (2014) 5988.
[17] Y.Y. Ren, G. Brown, A. Ródenas, S. Beecher, F. Chen, A.K. Kar, Opt. Lett. 37 (2012) 3339–3341.
[18] Y.Y. Ren, N.N. Dong, F. Chen, D. Jaque, Opt. Exp. 19 (2011) 5522–5527.
[19] F. Chen, Y. Tan, D. Jaque, Opt. Lett. 34 (2009) 28–30.
[20] F. Chen, J.R.V. de Aldana, Laser. Photon. Rev. 8 (2014) 251–275.
[21] K. Sugioka, Y. Cheng, Light Sci. Appl. 20 (2012) 4444–4453.
[22] K.M. Davis, K. Miura, N. Sugimoto, K. Hirao, Opt. Lett. 21 (1996) 1729–1731.
[23] A. Crespi, Y. Gu, B. Ngamsom, H.J.W.M. Hoekstra, C. Dongre, M. Polinau, R. Ramponi, H.H. van den Vlekkert, P. Watts, G. Cerullo, R. Osellame, Lab Chip 10 (2010) 1167–1173.
[24] N. Pavel, G. Salamu, F. Voicu, F. Jipa, M. Zamfirescu, T. Dascalu, Laser Phys. Lett. 10 (2013) 095802.
[25] S. Gross, N. Riesen, J.D. Love, M.J. Withford, Laser Photon. Rev. 8 (2014) L81–L85.
[26] J. Burghoff, S. Nolte, A. Tuennermann, Appl. Phys. A 89 (2007) 127–132.
[27] J. Thomas, M. Heinrich, P. Zeil, V. Hilbert, K. Rademaker, R. Riedel, S. Ringleb, C. Dubs, J. Ruske, S. Nolte, A. Tunnermann, Phys. Status Solidi (a) 208 (2011) 276–283.
[28] J. Siebenmorgen, T. Calmano, K. Pertermann, G. Huber, Opt. Express 18 (2010) 16035–16041.
[29] R. Osellame, M. Lobino, N. Chiodo, M. Marangoni, G. Cerullo, R. Ramponi, H.T. Bookey, R.R. Thomson, N.D. Psaila, A.K. Kar, Appl. Phys. Lett. 90 (2007) 241107.
[30] D.N. Nikogosyan, Theory of Dielectric Optical Waveguides, Academic, New York, 1974.